WRF Simulations of the 20-22 January 2007 Snow Events over Eastern Canada: Comparison with in-situ and Satellite Observations

J. J. Shi[1,2], W.-K. Tao[1], T. Matsui[1,2],R. Cifelli[7], A. Hou[3], S. Lang[1,4], A. Tokay[1,5], C. Peters-Lidard[6], G. Jackson[1], S. Rutledge[7], and W. Petersen[8]

[1]Laboratory for Atmospheres, NASA/Goddard Space Flight Center
Greenbelt, Maryland

[2]Goddard Earth Sciences and Technology Center, University of Maryland at Baltimore County, Baltimore, Maryland

[3]Goddard Modeling Assimilation Office NASA/Goddard Space Flight Center, Greenbelt, Maryland

[4]Science Systems and Applications, Inc., Lanham, Maryland

[5]Joint Center for Earth Systems Technology, University of Maryland Baltimore County, Baltimore, Maryland

[6]Laboratory for Hydrospheric Processes, NASA/Goddard Space Flight Center, Greenbelt, Maryland

[7]Department of Atmospheric Science, Colorado State University, Fort Collins, Colorado

[8]Earth Sciences Office, NASA/Marshall Space Flight Center, Huntsville, Alabama

Submitted to *J. Applied Meteor. Climatol.*

May 1, 2009

Corresponding author address: Dr. Jainn J. Shi, Code 613.1, NASA Goddard Space Flight Center, Greenbelt, MD 20771
E-mail: jainn.j.shi@nasa.gov.

Abstract

One of the grand challenges of the Global Precipitation Measurement (GPM) mission is to improve cold season precipitation measurements in middle and high latitudes through the use of high-frequency passive microwave radiometry. For this, the Weather Research and Forecasting (WRF) model with the Goddard microphysics scheme is coupled with a satellite data simulation unit (WRF-SDSU) that has been developed to facilitate over-land snowfall retrieval algorithms by providing a virtual cloud library and microwave brightness temperature (Tb) measurements consistent with the GPM Microwave Imager (GMI). This study tested the Goddard cloud microphysics scheme in WRF for two snowstorm events, a lake effect and a synoptic event, that occurred between 20 and 22 January 2007 over the Canadian CloudSAT/CALIPSO Validation Project (C3VP) site in Ontario, Canada.

The 24h-accumulated snowfall predicted by the WRF model with the Goddard microphysics was comparable to the observed accumulated snowfall by the ground-based radar for both events. The model correctly predicted the onset and ending of both snow events at the CARE site. WRF simulations capture the basic cloud properties as seen by the ground-based radar and satellite (i.e., CloudSAT, AMSU-B) observations as well as the observed cloud streak organization in the lake event. This latter result reveals that WRF was able to capture the cloud macro-structure reasonably well.

Sensitivity tests utilizing both the 2ice (ice and snow) and 3ice (ice, snow and graupel) Goddard microphysical schemes were also conducted. The domain- and time-average cloud species profiles from WRF simulations with both microphysical schemes show identical results (due to weak vertical velocities and therefore the absence of large precipitating liquid or ice particles like graupel). However, both microphysics schemes produced an appreciable amount of liquid water while the C3VP aircraft measurements show much less liquid water than the model in both snow events. These results indicate that additional research is needed to improve the current cloud microphysics scheme for

the extreme cold environment in high latitudes. Future aircraft observations are also needed to verify the abscence of graupel in high-latitude in-land snow events.

1. Introduction

The NASA Global Precipitation Measurement (GPM) mission is a multi-national, multi-satellite mission designed to provide a uniformly-calibrated precipitation measurement around the world. GPM consists of two components: a core satellite and a constellation of satellites. The core satellite carries a dual-frequency precipitation radar (DPR) and a microwave radiometric imager (GMI) with high-frequency capabilities. The constellation satellites consist of one NASA satellite, additional US satellite assets from NOAA and DMSP, and international satellites with passive microwave instruments. One of the major objectives of the GPM mission is to measure precipitation in middle and high latitudes over land during the cold season through the use of GMI high frequency radiometry and to further our understanding of precipitation processes at high latitudes. In 2007, a Canadian CloudSAT/CALIPSO Validation Project (C3VP) field campaign took place in south central Ontario, Canada. C3VP was a multi-national, multi-agency field experiment hosted by Environment Canada in and around the Centre for Atmospheric Research Experiments (CARE) about 80 km north of Toronto, Ontario. GPM's participation in C3VP was aimed at improving space-based snowfall detection and estimation algorithms (Peterson *et al.* 2007). For this study, the Weather Research and Forecasting (WRF) model with the Goddard microphysics scheme was utilized. WRF has also been coupled with a multi-sensor multi-frequency satellite simulator, the Goddard Satellite Data Simulation Unit (SDSU), for model evaluation and GPM algorithm support. The Goddard cloud microphysics scheme in WRF is tested for two distinct snowstorm events observed over the C3VP site in Ontario between 00 UTC 20 and 00 UTC 23 January 2007. Observations from the Environment Canada King radar, in-situ aircraft measurements, and CLOUDSAT are used to validate the model simulations

The Great Lakes of North America are unique water bodies capable of injecting enough warm water vapor into passing cold arctic air masses to produce snowstorms on their lee side during the fall and winter seasons. Under the right conditions, which are related to the lake-air temperature difference, airflow, and stability in the boundary layer,

strong organized convection may develop. The resulting lines or streaks of clouds streaming downwind of the lakes can produce considerable amounts of snow and constitute a lake effect snowstorm. In classic snowstorms (i.e., synoptic events), precipitation occurs in the cold air behind synoptic scale systems under stable conditions, which tend to suppress convection; however, lake enhancements of large synoptic scale storms can be significant, although associated convection seems to be weaker than that in lake effect storms caused by passing arctic air masses (Hjelmfelt 1990).

One of the simulated snow events examined in this study was a lake effect system. Although the dynamic mechanism of lake effect systems has been well studied (Brown 1972; Sykes and Henn 1989; Weckwerth *et al.* 1997, 1999; Kelly 1984; Cooper *et al.* 2000; Kristovich 1991; and Tripoli 2005) little detailed research on cloud microphysical properties in lake effect systems has been published (Schroeder *et al.* 2006). Schroeder *et al.* (2006) stated that one potential important factor in the development of heavy snowfall in lake effect events is the modification of the lake effect cloud and snow due to seeding from higher-level cloud layers. Evidence from aircraft microphysical measurements showed that microphysical snow-growth processes were locally enhanced within the convective boundary layer (CBL) clouds in seeded regions and the CBL was locally deeper in seeded regions than in non-seeded regions. They also analyzed ice-particle-size spectra to determine the microphysical differences between seeded and non-seeded areas. Seeded spectra in all cases implied more intense snowfall than their non-seeded counterparts. However, this "seeder-feeder" process has not been quantified for a lake effect event even though it's well known that in many non-lake-effect cases precipitation rates can be greatly increased by the "seeder-feeder" process. Due to the lack of numerical and observational studies of microphysical properties of lake effect systems, many questions still remain unresolved. It is not known if large precipitating particles like rain or graupel typically exist in these systems or if cloud liquid water exists in high latitude cloud systems during wintertime when the surface temperature is below -10^0C.

Table 1 lists the current as well as some past modeling studies (since 1990) of

lake effect snowstorms along with their cloud microphysics schemes. These studies focused more on the dynamical mechanisms of lake effect snowstorms than their cloud microphysical properties. When this study was initiated, no studies had been published that used WRF at high resolution (i.e., 1 km or finer, cloud resolving) to simulate high latitude snow events. One of the goals of this study is to determine whether a high-resolution WRF model with an advanced bulk microphysical scheme can properly simulate the cloud systems and snowfall associated with high-latitude snow events in inland environments.

A brief review of the WRF model, Goddard physical packages and satellite simulators is given in section 2. The synoptic situation for the period between 20 and 22 January 2007 is discussed in section 3. Section 4 discusses the design of the model simulations. In section 5, results from high-resolution WRF simulations using the Goddard cloud microphysics scheme for two distinct snowstorm events that observed over the C3VP site in Ontario between 00 UTC 20 and 00 UTC 23 January 2007 are compared with in situ and satellite observations, including the Environment Canada King City operational dual polarimetric radar located about 35 km southeast of the CARE site and CloudSAT-observed reflectivities. In addition, mean cloud hydrometeor profiles from the Goddard bulk microphysical scheme are compared with WRF's three other 3ice bulk microphysical schemes. The summary and conclusions are given in section 6.

2. WRF, the Goddard Physical Packages, and Satellite Simulators

WRF is a next-generation mesoscale forecast model and assimilation system. The development of WRF has been a multi-agency effort led by NCAR with several NOAA and DOD partners. The model is designed to support research advancing the understanding and the prediction of mesoscale precipitation systems, incorporating advanced numerics and data assimilation techniques, a multiple relocatable nesting capability, and improved physics. The WRF model has been used for a wide range of applications, from idealized research to operational forecasting, with an emphasis on horizontal grid sizes in the range of 1-10 km. WRF reflects flexible, state-of-the-art,

portable code that is efficient in computing environments ranging from massively-parallel supercomputers to laptops. Its modular, single-source code can be configured for both research and operational applications. Its spectrum of physics and dynamics options reflects the experience and input of the broad scientific community (Michalakes et al. 2004). The WRF Software Framework (WSF) provides the infrastructure wherein the dynamical solvers and physics packages interface with other solvers and programs for initialization, WRF-Var, and WRF-Chem. There are two dynamics solvers in the WSF: the Advanced Research WRF (ARW) solver (originally referred to as the Eulerian mass or "em" solver) developed primarily at NCAR, and the NMM (Nonhydrostatic Mesoscale Model) solver developed at NCEP. Community support for the former is provided by the MMM Division of NCAR and that for the latter is provided by the Developmental Testbed Center (DTC). Detailed documentation for WRF and WSF can be found in Skamarock et al (2008). In this study, the ARW version of WRF was used.

Various Goddard physical packages (i.e., CRM-based microphysics, radiation and land-surface hydrology processes) and a real-time forecast system using GEOS global analyses that was developed at NASA have recently been implemented into the WRF ARW system (Fig. 1a). The Goddard Cumulus Ensemble (GCE) model's (Tao and Simpson 1993) one-moment bulk microphysical scheme was recently implemented into WRF. This scheme is mainly based on Lin *et al.* (1983) with additional processes from Rutledge and Hobbs (1984). The Goddard microphysical scheme includes three different options, 3ice-graupel, 3ice-hail, and 2ice (only cloud ice and snow). The Goddard microphysics scheme was recently modified to reduce over-estimated and unrealistic amounts of cloud water and graupel in the stratiform region (Tao *et al.* 2003; Lang *et al.* 2007; Tao *et al.* 2009).

The Goddard radiation package includes both longwave and shortwave effects; for two decades it was developed at NASA Goddard for use in general circulation, regional and cloud-resolving models (Chou and Suarez 1999, 2001). A few recent improvements were done before the Goddard radiation package was added into WRF: 1) the shortwave radiation code was optimized for computational speed (improved by a

factor of two), 2) cloud optical properties were made to be consistent to the assumptions in Goddard microphysics, 3) stratospheric layers can be optionally added above the top of the model's uppermost pressure level, and 4) the direct effect of aerosols on both longwave and shortwave radiation were accounted for (Matsui et al. 2007). The CRM-based physics package has improved forecasts (i.e., simulations) of convective systems (Tao et al 2009).

The Goddard Satellite Data Simulation Unit (SDSU) is an end-to-end multi-satellite simulator unit. It has six simulators at present: passive microwave, radar, visible-infrared spectrum, lidar, ISCCP type, and broadband. The SDSU can compute satellite-consistent radiances or backscattering signals from simulated atmospheric profiles and condensates consistent with the Goddard microphysics (Fig. 1b). For example, it can generate estimates of retrieved microphysical quantities that can be directly compared with high-resolution satellite (i.e., TRMM, CloudSat) products. These simulated radiances and backscattering can be directly compared with satellite observations, establishing a satellite-based framework for evaluating the cloud parameterizations. This method is superior to the traditional method of validating models with satellite-based products, since models and satellite products often use different assumptions in their cloud microphysics (Matsui *et al.* 2009). Once the cloud model reaches satisfactory agreement with the satellite observations, simulated clouds, precipitation, atmospheric states, and satellite-consistent radiances or backscattering will be provided to the science team as an a priori database for developing physically-based cloud and precipitation retrieval algorithms. Thus, the SDSU coupled with the multi-scale modeling system (of which WRF is one component) can allow for a better understanding of cloud processes as well as provide a means to improve precipitation retrievals for current and future NASA satellite missions (Matsui et al. 2008).

3. Synoptic Conditions

There were two significant snow events during the 72h period from 00 UTC 20 to 00 UTC 23 January 2007. On 20 January 2007, a cold front passed the Toronto area

from the north in association with an upper level trough centered over eastern Canada. The passage of the cold front produced northwesterly flow near the surface, allowing for the development of isolated snow bands in the lee of the Georgian Bay of Lake Huron. A series of NW-SE oriented snow bands developed over the CARE site (79.78^0W and 44.23^0N) after 00 UTC on 20 January. Although the bands persisted throughout the day, the nearby King radar (located at 79.57^0W, 43.96^0N) observations showed that they were most intense prior to 06 UTC (isolated cores exceeding 30 dBz) with echo tops below about 3 km AGL. Fig. 2a shows the 24h accumulation of SR (liquid equivalent snow rate). Most of the intense snowfall was between Lake Hudson and the CARE site with the 24h SR accumulations ranging from 2 to >20 mm. Daily accumulations measured from the DFIR (double fenced international reference) gauge at the CARE site indicated approximately 12.3 mm of SR for the event, which was the highest daily amount observed for the entire 2006-2007 season (Bringi et al. 2008). Because the snowfall for this first event was mostly caused by cold air passing over the relatively warm lake surface, this event is hereafter called the *lake event*.

In contrast to the first snow event on 20 January, the second snow event on 22 January was a result of a synoptic-scale cold frontal passage across southern Ontario. The 22 January event developed in response to the passage of a 500-mb short wave trough and an associated surface low across the C3VP domain between 00 and 12 UTC (Petersen et al. 2007). This synoptic scale system was associated with widespread light to moderate snowfall (Fig. 2b). King radar data showed that precipitation entered the western portion of the domain around 15 UTC on 21 January. Initially, the precipitation echoes weakened considerably as the system moved eastward and northeastward. However, radar imagery showed that a weak, mesoscale snow band propagated northward in the vicinity of the CARE site and interacted with the larger-scale system after about 21 UTC on 21 January. The combined system continued to move eastward and left the C3VP domain after 08 UTC on 22 January. Range Height Indicator (RHI) scans from the King radar indicated that echo tops ranged up to about 5.5 km AGL and that reflectivities were mostly below 25 dBZ. Surface temperatures during this event were well below freezing, -9^0C to -10^0C, and rawinsonde data collected during the event

indicated near water-saturated conditions (and definitely ice supersaturated conditions) in the first several km of the sounding. Winds were generally moderate at the surface, on the order of 5 ms^{-1}, for the duration of the event. The DFIR at the CARE site reported about 2.4 mm of 24h accumulated SR associated with this event (Bringi et al. 2008). This snow event is hereafter referred to as the *synoptic event*.

4. Design of Model Simulations

NASA's interest in the Canadian CloudSat/CALIPSO validation project (C3VP) was primarily to support over-land snowfall retrievals using high frequency radiometer observations through a set of ground- and aircraft-based instrumental and remote sensing measurements as well as high-resolution numerical modeling. During the winter of 2006-2007, a number of in-situ and remote sensing precipitation measuring devices were operated at the Center of Atmospheric Research Experiment (CARE) site located near Egbert, Ontario about 30 km to the NW of the King City C-band operational dual-polarized radar. While the experiment was originally designed to measure winter precipitation for C3VP, the NASA's Global Precipitation Measurement (GPM) ground validation program joined the efforts (Petersen et al., 2007) bringing the 2D-video and Parsivel Disdrometers and a multi-frequency radar to the CARE site. To examine the cloud dynamics and microphysical properties of the snowstorms, WRF v2.2.1 with the Goddard microphysical scheme was used to conduct the simulations. In this study, only 3ice-graupel and 2ice options were used with WRF. For comparison, other 3ice bulk microphysical schemes (Purdue-Lin, WSM6 and Thompson, see the details in Skamarock et al (2008)) in WRF V2.2.1 are tested and examined in the same case studies.

Triple nested domains were constructed with horizontal grid spacing of 9, 3 and 1 km, with corresponding numbers of grid points 301 x 41, 430 x 412, and 457 x 457, respectively (Fig. 3). Terrain-following vertical coordinate with 61 layers was constructed with resolutions ~5-10 mb inside the PBL and ~20-25 mb above the PBL. Time steps of 30, 10 and 3.333 seconds were used in these nested grids, respectively. The coarse domain covered from Nebraska, US to Nova Scotia, Canada, from Virginia,

US to the northern end of Ontario, Canada, while the finest domain covers the most of the southeastern part of Ontario and includes most of Lake Huron and Erie (Fig. 3). The model was initialized from NOAA/NCEP global analyses (1.0^{o} by 1.0^{o}). Time-varying lateral boundary conditions also from NOAA/NCEP global analyses were provided at 6-h intervals. The model was integrated for 48 hours twice from 12UTC 19 to 12UTC 21 and from 00UTC 21 to 00 UTC January 2007 respectively, in order to cover both snow events.

The Grell-Devenyi ensemble cumulus parameterization scheme (Grell and Devenyi, 2002) was used for the coarse 9 km grid domain. The cumulus parameterization scheme was turned off in the 3 and 1 km grid domains while the Goddard cloud microphysics scheme was used in all three grid domains. The Goddard longwave and shortwave schemes recently added into WRF and discussed in Section 2 were adopted to provide longwave and shortwave parameterizations that interact with the atmosphere. The planetary boundary layer parameterization employed the Mellor-Yamada-Janjic (Mellor and Yamada 1982, and coded/modified by Dr. Janjic for NCEP Eta model) Level 2 turbulence closure model through the full range of atmospheric turbulent regimes. The surface heat and moisture fluxes (from both ocean and land) were computed from similarity theory (Monin and Obukhov 1954). The Noah land surface model is based on Chen and Dudhia (2001). It is a 4-layer soil temperature and moisture model with canopy moisture and snow cover prediction. It provides sensible and latent heat fluxes to the boundary layer scheme.

5. Results

5.1 Snowfall comparison

Fig. 4 shows the 24h-accumulated snowfall (mm, liquid water equivalent, LWE) from the inner (1-km) domain of the WRF output for (a) the lake event and (b) the synoptic event. For a better comparison with Fig. 2, both Fig. 4a and 4b are centered at the King radar site (79.57^{0}W and 43.96^{0}N). Both figures also cover 201 grid points (200

km) in the longitude and latitude directions similar to the 100-km radius used in Fig. 2. Figs. 2a and 4a represent the LWE of the 24h snowfall (between 00 UTC 20 and 00 UTC 21 January 2007) from the King radar observation and the WRF model simulation for the lake event respectively, while Figs. 2b and 4b cover the 24h period from 12 UTC 21 to 12 UTC 22 January 2007 for the synoptic event. For both the lake and synoptic events, the 1-km domain with the Goddard microphysics produced a comparable amount of [1]snowfall across the region as observed by the King radar[1], 12.5-15 mm LWE for the lake event and 2.5-5 mm LWE for the synoptic event. However, the heavy snowfall region in the model simulation for the lake-effect event is about ~0.2^0 west of the one shown in the King radar observation. The 1-km model simulation also produced a slightly larger snowfall (5-7.5 mm LEW) region west of Lake Ontario while the King radar observation only shows some small spotty locations with 5-7.5 mm LWE just west of the CARE site.

The PDF (probability distribution function) of 24h-accumulated snowfall (LWE) from both the model simulation and the observation of the King radar is shown on Fig. 5. The result reveals that the 24h-accumulated snowfall predicted by the model agrees well with the observation of the King radar throughout the whole spectrum for the lake event. For the synoptic event, most of the snowfall predicted by the model is in the 2.0-4.0 mm range (more than 80%), while most of the snowfall observed by the King radar is in the 0.5-2.0 mm (43%) and 2.0-4.0 (55%) mm. The King radar observed only 2% of grid points with snowfall in the 4.0-6.0 mm range and none with snowfall larger than 6.0 mm, while the model predicted around 10% of grid points with snowfall in the 4.0-6.0 mm range. Overall, both the model prediction and the King radar observation show that there are almost 10% of grid points with snowfall greater than 6.0 mm in the lake event, while virtually no grid point with snowfall larger than 6.0mm in the synoptic event. This confirms that the synoptic event produced more uniformly distributed snowfall in the region while the lake event produced strong snowfall at the grid points right under the cloud streak.

[1]The methodology used to derive liquid equivalent snowfall from the King radar is described in Huang et al. 2009

Figs. 6 show the 72h time series of snowfall rates (mm/hr) at the CARE site (79.78^0W, 44.23^0N) for the period between 00UTC 20 and 00 UTC 23 January 2007. Fig. 6a represents the data collected from the Parsivel (Laser Optical) Disdrometer stationed at the CARE site, while Fig. 6b represents the model simulation at the same location. As shown in Fig. 6, the heavy snowfall at the CARE site for the lake-effect event started around 03 UTC and ended around 07 UTC with light snowfall throughout the rest of January 20. For the synoptic event, the snowfall started at 02 UTC and ended around 08 UTC on January 22. Comparing Figs. 6a and 6b, the onset and ending time predicted by the model agree well with the observation, especially the model also predicted the correct time of the peak snowfall. As pointed out in Bringi et al. (2008), snow fell at the CARE site during the lake event was particularly dry with the density possibly between 0.06 and 0.08 g/cm^3. With the snowfall number observed by the Parsivel Disdrometer divided by a number between 12 and 16 to convert the snowfall depth to the LWE, snowfall predicted by the model for the lake event is still much weaker than the Parsivel Disdrometer observation. However, this is easily understandable when comparing Figs. 2 and 4. The model predicted intense snowfall region is about 0.2^0 west of the CARE site and the model did not predict strong snowfall at the CARE site. On other hand, snowfall predicted by the model for the synoptic event is comparable to the Parsivel Disdrometer observation.

Overall, the amount of accumulated snowfall predicted by the model across the region agrees well with the King radar observation in both events, except that the model didn't predict intense snowfall at the CARE site. The model correctly predicted the onset and ending of both snow events as shown in the Parsivel Disdrometer observation at the CARE site. Although the model did not predict the correct snowfall rate at the CARE site, it is extremely difficult to predict an accurate precipitation at a single-point location in a high-resolution mesoscale model simulation, and may requires alternative method like the composite-based method used in Nachamkin et al. (2005) to evaluate it.

5.2 Comparison between model-simulated radar reflectivity and observations from King Radar and CloudSAT CPR

For the lake event (Fig. 7), the cloud streak simulated by the model is in good agreement with the observed in terms of the timing (near 03 UTC 20 Jan 2007) and location; however, the observed cloud streak seems to be oriented more north-south and the model-predicted C-band reflectivities are about 10-dbz stronger than the observed ones from King Radar. Observed echo tops reach to around 3.5 km while those in the model only reach to around 2.5 km. CloudSAT-observed radar (94GHz) reflectivities also confirm the presence of cloud with the 3.5 km echo tops (see Fig. 9). Fig. 8 shows that the model-simulated C-band radar reflectivity for the synoptic event is also in good agreement with the observed in terms of the strength and vertical structure. However, the model-simulated reflectivity shows a larger strong reflectivity area (>20 dBz) than the observed. Both the model and observed reflectivity cross-sections show radar echoes extending to around 4 km except for a few spikes that go above 4 km in the observed reflectivity cross-section.

Fig. 9 displays W-band radar reflectivities from CloudSAT Cloud Profiling Radar (CPR) observations. W-band radar reflectivities are simulated from the radar simulator (Masunaga and Kummerow 2005) in the SDSU using the WRF simulated atmosphere profiles along the exact CloudSat overpass point. Pass 1 represents the lake event while Passes 2 and 3 represent the early and late stages of the synoptic event. Note that the WRF output is every 1hr due to its volumetric size and the timing of simulated reflectivities is the closest much within 30min window. The cross-sectional comparison indicates that WRF successfully captured the spatial distribution of radar reflectivities in low clouds (pass 1), large-scale nimbostratus (pass 2), and overlapped clouds (pass 3). The statistical comparison (contoured frequency with altitude diagrams, CFADs, Fig. 10) shows that WRF-SDSU overestimated radar reflectivities above 4 km in Pass 3 and throughout the whole column in Pass 2. In Pass 1, distributions of WRF-SDSU radar reflectivities seem to be comparable to CloudSat radar reflectivities throughout the whole spectrum except that WRF-SDSU radar reflectivity only reaches around 2.5km. This result demonstrates that WRF (with Goddard bulk one-moment microphysics) was able to capture the cloud macro-structure reasonably well but not the cloud microphysics. An

improved version of the one-moment bulk microphysics is now being developed based largely on the radiance-based model evaluations here and C3VP aircraft in-situ observations of microphysics (A. Heymsfiueld 2009, personal communication). In addition, finer spatial resolutions (than the current 1-km horizontal grid spacing) may be required so that simulations can realistically represent the evolution of less vigorous cold cloud systems. Improved microphysics and hence model simulations are necessary to provide consistent 4D thermodynamic and dynamic cloud data sets for future GPM snow retrievals and to improve our understanding of precipitation processes over high-latitude regions.

5.3 Comparison between model simulated brightness temperatures and AMSU-B observations

We have also simulated high-frequency microwave brightness temperature (Tb) for Advanced Microwave Sounding Unit –B (AMSU-B) sensors. AMSU-B sensors were originally designed for temperature and humidity profile retrievals. However, these high-frequency channels (150.00, 183.31±1, 183±31, and 183.31±7GHz) were found to be sensitive for falling snow and relatively insensitive to ground signals. Therefore, they are useful for over-land snowfall retrieval (Skofronick-Jackson et al. 2004). GPM Microwave Imager (GMI) plan to includes such high-frequency channels to support over-land snowfall retrievals over mid- and high-latitude regions. Thus, we are encouraged to simulate and evaluate the high-frequency Tb from the WRF simulations to support GPM missions. AMSU-B-consistent Tbs were computed from the WRF simulations through a passive microwave simulator in the SDSU (delta-Eddington two-stream radiative transfer with slant path view, Kummerow 1993; Olson and Kummerow 1996). AMSU-B Tbs (within the 30-degree sensor-viewing angle) and corresponding Tbs simulated from the WRF simulation were sampled consistently in time (± 30min) and space (IFOV=16.4km at nadir).

A total of 10 AMSU-B swaths were matched containing 1738 and 2958 Tb samples over water and land, respectively (Fig 11). These were then used to evaluate the

simulated cold cloud systems for various Tbs. Tbs of 150 GHz have the largest discrepancy (RMSE=10.2 over water and RMSE=9.93 over land) between the observations and simulation due to uncertainties in the simulated surface properties (e.g., skin temperature and surface emissivity), which were not well parameterized in the SDSU currently. Tbs of 180.31±1GHz and 180.31±3GHz have stronger water absorption channels; hence simulated Tbs are essentially unaffected from surface properties. As a result, Tbs between the observations and the simulation have less discrepancy. Tbs of 180.31±7GHz have the highest correlation (0.84) among the different channels. It is interesting to note that the simulation tends to overestimate Tbs of 150 GHz and 180.31±7GHz (where the atmosphere is more transparent), while it tends to underestimate Tbs of other channels (where the atmosphere is less transparent). This suggests that there might be discrepancies between the simulated and actual temperature and humidity profiles. Additional model simulations with higher resolution and improved microphysics as well as better representation of surface characteristics will be conducted in the near future.

5.4 Vertical profiles of cloud species from Goddard cloud microphysics scheme

Fig. 12 shows vertical profiles of the domain- and time-averaged cloud species for using the Goddard 3ICE-graupel and 2ICE schemes. In the figures, Qcloud represents cloud liquid water (smaller particle) and Qrain for cloud rain water (larger particle). For the lake event (Figs 12a and 12b), large precipitating particles (rain and graupel) did not form for either experiment because the simulated vertical velocities were weak (~50 cm/s) and extreme cold temperature (see Fig. 14). Identical profiles for cloud water, cloud ice and snow for both experiments were simulated even though the 3ICE-graupel scheme contains physics that allows the production of graupel. Also note the presence of cloud water during this snow event. This feature has both been observed and simulated (e.g., a snow event over Japan Sea). C3VP aircraft observations also suggested that there was a little liguid water during the event observed by the C3VP aircraft measurements (A. Heymsfiueld 2009, personal communication). It is also apparent that all cloud species were capped below 700mb indicating that the lake event was mostly a PBL phenomenon

as mentioned by many past studies (Kristovich 1993; Weckwerth 1999; Cooper et al 2000; Tripoli 2005).

The same vertical profiles of the domain- and time-averaged cloud species for the synoptic event are presented in Figs 12c and 12d. Similar to the lake event, The Goddard 3ICE-graupel and 2ICE schemes produced identical vertical profiles without large precipitating particles (rain and graupel). Both Goddard schemes produced much cloud snow below 500 mb and cloud ice between 400 and 700 mb. Both schemes produced certain amount of liquid cloud water although there was a little liguid water during the synoptic event observed by the C3VP aircraft measuremnts (A. Heymsfield 2009, personal communication). The cloud water (Qcloud) production is about one-third of the cloud snow (Qsnow) production near 950-mb level while it is only about one-tenth in the C3VP aircraft observations near 1-km height (Fig. 13). Why did the model produce larger liquid/ice water ratio? It is possible that the Goddard cloud microphysics scheme in WRF may have allowed too much condensation. In a separated sentivity test (not shown here), the liquid water production was decreased when the condensation was reduced. Another reason may be that the fly path of aircraft did not go through the entire WRF domain (especially the southern one-third where cloud liquid water existed) and was mostly around the CARE site. Fig. 14 shows the N-S cross-section of temperature and cloud ice-plus-snow fields along ~81^0W line. The air was very cold (< -9^0C) throughout the whole air column in both events. It is also easy to understand why there was only a little super-cooled liquid in both lake and synoptic events observed by the C3VP airecraft observation. This punctuates that the Goddard cloud microphysics scheme may need further tuning to reduce the production of liquid water for high-latiude snow events. Fig. 14a also demonstartes the cloud streak structure in the lake event while the same streak structure ddesn't exist in the synoptic event (Fig. 14b).

6. Summary and future work

One of the grand challenges of the Global Precipitation Measurement (GPM) mission is to improve precipitation measurements in mid- and high-latitudes during cold

seasons through the use of high-frequency passive microwave radiometry. For this, the Weather Research and Forecasting (WRF) model with the Goddard microphysics scheme is coupled with a Satellite Data Simulation Unit that has been developed to facilitate over-land snowfall retrieval algorithms by providing a virtual cloud library and microwave brightness temperature (Tb) measurements consistent with the GPM Microwave Imager (GMI). This study tested the Goddard cloud microphysics schemes (2ICE and 3ICE with graupel) in WRF for two snowstorm events (January 20-22, 2007) that took place over the C3VP site up in Ontario, Canada. It should also be noted that there was no published high-resolution (1 km or finer) simulation study using WRF with cloud resolving capability for any high latitude snow event when this study was started. This study has demonstrated the feasibility of using WRF with Goddard microphysical scheme in a cloud resolving scale for high-latitude snow events.

The 24h-accumulated snowfall predicted by the WRF model with the Goddard microphysics was comparable to the King radar observed accumulated snowfall for both events. However, the WRF model failed to predict the intense snowfall at the CARE site because that the intense snowfall region predicted by the WRF model was roughly 0.2^0 west of the region observed by the King radar. The PDF analysis of the accumulated snowfall reveals that results from the WRF model agrees well with the observation of the King radar in both events. The model correctly predicted the onset and ending of both snow events. Although the model did not predict the correct snowfall rate at the CARE site, it is extremely difficult to predict an accurate precipitation at a single-point location in a high resolution mesoscale model.

In this study, the radar reflectivity forecasted by the WRF model was compared against the radar and satellite observations. Preliminary WRF simulations capture the basic cloud properties as seen by ground-based radar and satellite (i.e., CloudSAT, AMSU-B) observations and also demonstrate the cloud streak feature in the lake event. However, the model under predicts the echo top heights for the lake event. WRF simulations also capture the 2-layer cloud structure during the late stage of the synoptic

event. This result reveals that WRF was able to capture the cloud macro-structure reasonably well but not the cloud microphysics.

WRF simulations with two different Goddard microphysical schemes (3ICE and 2ICE scheme) show identical results (due to weak vertical velocities and therefore the absence of large precipitating liquid or ice particles like graupel). Both Goddard cloud microphysics schemes in WRF produced certain amount of liquid water while the C3VP aircraft measurements show there was much less liquid water than the model produced in the synoptic event. One sensitivy test reveals that there could be too much condensation occured in the model. The domain-averaged statistics may be partially inappropriate to a direct comparison with the aircraft measurements due to the fly path of aircraft not covering the entire WRF domain (especially the southern one-third). Future research is needed to fine-tune the current cloud microphysics scheme for the extreme cold environment in high latitudes. Although the model reveals that there was no graupel in either lake or synoptic event due to the weak vertical velocity in the events, there was no observation to confirm this. Future aircraft observations are needed to verify the non-existence of graupel in high-latitude in-land snow events. This numerical study also confirms cloud streraks in the lake event were relatively shallow and it was mainly a PBL event as mentioned in many past studies (Kristovich 1993; Weckwerth 1999; Cooper et al 2000; Tripoli 2005).

Note that model data can often be used to infer critical cloud information/properties that are not directly observable by satellites. The linkage between the satellite and model data usually depends on simulated Tbs (brightness temperatures). As such, an accurate vertical distribution of cloud species is important for satellite retrievals. Unrealistic precipitation ice contents (i.e., snow and graupel) and particle size distribution, for example, can bias the simulated Tbs and reflectivities making it difficult to infer cloud properties from remote sensing data by linking them with synthetic values from models. Also note that cloud ice and cloud water are important cloud species for cloud-radiation interaction. For future research, WRF simulations using higher-resolution initial conditions (NCEP Eta 32 km), more and higher vertical resolution (lower and

upper troposphere), improved microphysics and sensitivity of planetary boundary layer (PBL) processes will be conducted. In addition, a WRF-Earth satellite simulator with realistic ground emissivity is required in a passive microwave simulator in the SDSU.

7. Acknowledgement

The WRF-Goddard cloud microphysics coupling is supported by the NASA Headquarters Atmospheric Dynamics and Thermodynamics Program and the NASA Tropical Rainfall Measuring Mission (TRMM). The authors are grateful to Dr. R. Kakar at NASA headquarters for his support of this research. The authors appreciate the useful discussion with Dr. Andy Heymsfield. The authors also want to thank Dr. Nai-Yu Wang of University of Maryland for providing plots of ice and liquid water vertical profiles from the C3VP aircraft measurements.

8. References

Ballentine, R. J., A. J. Stamm, and E. E. Chermack, 1998: Mesoscale model simulation of the 4-5 January 1995 lake-effect snowstorm. *Wea. and Forecasting*, **13**, 893-920.

Bringi, V. N., G.-J. Huang, D. Hudak, R. Cifelli, S. Rutledge, 2008: A methodology to derive radar reflectivity – liquid equivalent snow rate relations using C-band radar and a 2D video disdrometer. The 5th European Conference on Radar in Meteorology and Hydrology, 30 June - 4 July 2008, Helsinki, Finland.

Brown, R. A., 1972: On the inflection point instability of a stratified Ekman boundary layer. *J. Atmos. Sci.*, **29**, 850–859.

Chen, F., and J. Dudhia, 2001: Coupling an advanced land-surface/ hydrology model with the Penn State/ NCAR MM5 modeling system. Part I: Model description and implementation. Mon. Wea. Rev., **129**, 569–585.

Chou M.-D., and M. J. Suarez, 1994: An efficient thermal infrared radiation parameterization for use in general circulation models. NASA Tech. Memo. 104606, 3, 85pp.

Chou M.-D., and M. J. Suarez, 1999: A solar radiation parameterization for atmospheric studies. NASA Tech. Rep. NASA/TM-1999-10460, vol. 15, 38 pp

Chou M.-D., and M. J. Suarez, 2001: A thermal infrared radiation parameterization for atmospheric studies. NASA/TM-2001-104606, vol. 19, 55pp

Cooper, K. A., M. R. Hjelmfelt, D. A. R. Kristovich, N. F. Laird, and R. G. Derickson, 2000: Numerical simulations of convective rolls and cells in lake-effect snow bands. *Mon. Wea. Rev.*, **128**, 3283–3295.

Grell, G. A., and D. Devenyi, 2002: A generalized approach to parameterizing convection combining ensemble and data assimilation techniques. Geophys. Res. Lett., **29(14),** Article 1693.

Hjelmfelt, M. R., 1990: Numerical study of the influence of environmental conditions on lake effect snowstorms over Lake Michigan. *Mon. Wea. Rev.,* **118,** 138–150.

Huang, G-J., V. N. Bringi, R. Cifelli, D. Hudak, and W. A. Petersen, 2009: A methodology to derive radar reflectivity – liquid equivalent snow rate relations using C-band radar and a 2D video disdrometer. *J. Atmos. Oceanic Technol.*, conditionally

accepted

Kelly, R. D., 1984: Horizontal roll and boundary-layer interrelationships observed over Lake Michigan. *J. Atmos. Sci.*, **41**, 1816–1826.

Kristovich, D. A. R., 1991: The three-dimensional flow fields of boundary layer rolls observed during lake-effect snowstorms. Ph.D. thesis, University of Chicago, 182 pp. 1359.

——, 1993: Mean circulations of boundary-layer rolls in lake-effect snow storms. *Bound.-Layer Meteor.,* **63,** 293–315.

Kummerow, C., 1993: On the accuracy of the Eddington approximation for radiative transfer in the microwave frequencies. *J. Geophys. Res.*, **98**, 2757-2765.

Olson W. S., and C. D. Kummerow, 1996: Simulated retrieval of precipitation profiles from TRMM Microwave Imager and precipitation radar data. Preprints, *Eighth Conf. on Satellite Meteorology and Oceanography,* Atlanta, GA, Amer. Meteor. Soc., 248–251.

Lang, S., W.-K. Tao, R. Cifelli, W. Olson, J. Halverson, S. Rutledge, and J. Simpson, 2007: Improving simulations of convective systems from TRMM LBA: Easterly and westerly Regimes. *J. Atmos. Sci.*, **64**, 1141-1164.

Lin, Y.-L., R. D. Farley and H. D. Orville, 1983: Bulk parameterization of the snow field in a cloud model. *J. Clim. Appl. Meteor.*, **22**, 1065-1092.

Masunaga, H., and C.D. Kummerow, 2005: Combined Radar and Radiometer Analysis of Precipitation Profiles for a Parametric Retrieval Algorithm. *J. Atmos. Oceanic Technol.*, **22**, 909–929.

Matsui, T., W.-K. Tao, and J.-J. Shi, 2007; Goddard radiation and aerosol direct effect in Goddard WRF, NASA/UMD WRF workshop, UMD, college park, Sep 14, 2007.

Matsui, T., W. Tao, J. Chern, X. Zeng, X. Li, J. J. Shi, S. Lang, B. Shen, H. Masunaga, 2008: Goddard Satellite Data Simulation unit: A comprehensive multi-sensor satellite simulators for supporting satellite missions. AGU 2008 Fall Meeting, American Geophysical Union, San Francisco, California, December 15-19, 2008.

Matsui, T., X. Zeng, W.-K. Tao, H. Masunaga, W.S. Olson, and S.E. Lang, 2009; Evaluation of long-term cloud-resolving model simulations using satellite radiance observations and multi-frequency satellite simulators, *Journal of Atmospheric and*

Oceanic Technology (in press).

Mellor, G. L., and T. Yamada, 1982: Development of a turbulence closure model for geophysical fluid problems. *Rev. Geophys. Space Phys.*, **20**, 851–875.

Michalakes, J., J. Dudhia, D. Gill, T. Henderson, J. Klemp, W. Skamarock, and W. Wang, 2004: The Weather Research and Forecast Model: Software architecture and performance. The 11th ECMWF Workshop on the Use of High Performance Computing in Meteorology. 25–29 October 2004, Reading, U.K., Ed. George Mozdzynski.

Monin, A.S. and A.M. Obukhov, 1954: Basic laws of turbulent mixing in the surface layer of the atmosphere. Contrib. Geophys. Inst. Acad. Sci., USSR, **151**, 163–187 (in Russian).

Nachamkin, J. E., S. Chen, and J. Schmidt, 2005: Evaluation of Heavy Precipitation Forecasts Using Composite-Based Methods: A Distributions-Oriented Approach. *Mon. Wea. Rev.*, **133**, 2163–2177.

Peterson, W. A., D. Hudak, V. N. Bringi, P. Siqueira, A. Tokay, V. Chandrasekar, L. F. Bliven, R. Cifelli, T. Lang, S. Rutledge, G. Skofronick-Jackson, and M. Schwaller, 2007: NASA GPM/PMM Participation in the Canadian CloudSAT/Calipso Validation Project (C3VP): Physical process studies in snow. The 33rd International Conference on Radar Meteorology, American Meteorological Society, 6-10 August 2007, Cairns, Australia.

Rao, G.-S., E. and M. Agee, 1996: Large eddy simulation of turbulent flow in a marine convective boundary layer with snow. *J. Atmos. Sci.*, **53**, 86-100.

Rutledge, S.A., and P.V. Hobbs, 1984: The mesoscale and microscale structure and organization of clouds and precipitation in mid-latitude clouds. Part XII: A diagnostic modeling study of precipitation development in narrow cold frontal rainbands. *J. Atmos. Sci.*, **41**, 2949-2972.

Schroeder, J. J., D. A. R. Kristovich, and M. R. Hjelmfelt, 2006: Boundary layer and microphysical influences of natural cloud seeding on a lake-effect snowstorm. *Mon. Wea. Rev.*, **134,** 1842-1858.

Shamarock, W. C., J. B. Klemp, J. Dudhia, D. Gill, D. Barker, M. Duda, X.-Y. Huang, W. Wang, and J.G. Powers, 2008: A description of the advanced research WRF Version 3. *NCAR Technical Note NCAR/TN-475+STR*, Boulder, Colorado.

Skofronick-Jackson G. M., M.-J. Kim, J. A. Weinamn, and D.-E. Chang, 2004: A physical model to determine snowfall over land by microwave radiometry. IEEE Trans. *Geosci. Remote Sens.*, **42**, 1047–1058.

Sykes, R. I., and D. S. Henn, 1989: Large-eddy simulation of turbulent sheared convection. *J. Atmos. Sci.*, **46**, 1106–1118.

Tao, W.-K., and J. Simpson, 1993: The Goddard Cumulus Ensemble Model. Part I: Model description. *Terrestrial, Atmospheric and Oceanic Sciences,* **4**, 19-54.

——, J. Simpson, D. Baker, S. Braun, M.-D. Chou, B. Ferrier, D. Johnson, A. Khain, S. Lang, B. Lynn, C.-L. Shie, D. Starr, C.-H. Sui, Y. Wang and P. Wetzel, 2003: Microphysics, radiation and surface processes in the Goddard Cumulus Ensemble (GCE) model, *A Special Issue on Non-hydrostatic Mesoscale Modeling, Meteorology and Atmospheric Physics,* **82**, 97-137.

——, J. J. Shi, S. Chen, S. Lang, S.-Y. Hong, G. Thompson, C. Peters-Lidard, T. Matsui, A. Hou, S. Braun, and J. Simpson, 2009: Studying precipitation processes in WRF with Goddard bulk microphysics: Comparison with different microphysical schemes. *Mon. Wea. Rev.*, **(submitted).**

Tripoli, G. J., 2005: Numerical study of the 10 January 1998 lake-effect bands observed during Lake-ICE. *J. Atmos. Sci.*, **62**, 3232-3249.

Weckwerth, T. M., J. W. Wilson, R. M. Wakimoto, and N. A. Crook, 1997: Horizontal convective rolls: Determining the environmental conditions supporting their existence and characteristics. *Mon. Wea. Rev.*, **125**, 505–526.

——, T. W. Horst, and J. W. Wilson, 1999: An observational study of the evolution of horizontal convective rolls. *Mon. Wea. Rev.*, **127**, 2160–2179.

List of Table and Figures

observations from three different passes and the right panels are the WRF-simulated.

Fig. 10 Instantaneous contoured frequency with altitude diagrams (CFADs) of CloudSAT-observed and WRF-SDSU-simulated Cloud Profiling Radar (CPR, 94 GHz) reflectivity. Left panels show the CloudSAT observations from three different passes and the right panels are the WRF-simulated.

Fig. 11 Scatter plots between AMSU-B-observed and WRF-SDSU-simulated Tbs at different high-frequency channels. Red (blue) points represent over-land (water) points. Root Mean Square Error (RMSE) and correlation (COR) are also displayed.

Fig. 12 WRF simulated vertical profiles of domain- and 24-hour time-average cloud species (i.e., cloud water, rain, cloud ice, and snow) for the lake event using (a) the GCE-3ice scheme, and (b) GCE-2ice scheme for the 24-hour period covering from 00UTC January 20 to 00UTC January 21, 2007, and for the synoptic event (c) the GCE-3ice scheme, and (d) GCE-2ice scheme for the 24-hour period covering from 00UTC January 21 to 00UTC January 22, 2007.

Fig. 13 Vertical profiles of C3VP aircraft measurement of ice and liquid water content between 0600UTC and 0624UTC January 22, 2007.

Fig. 14 WRF simulated temperature (^{0}C), cloud ice (g/m^3) and cloud snow (g/m^3) profiles for (a) the lake and (b) the synoptic events.

	Modeling System	Microphysics	Resolution	Simulated Hours
Hjelmfelt 1990	CSU Mesoscale model (Pielke 1974, 1984; McNider and Pielke 1981)	Hjelmfelt & Braham (1983) Mahrer & Pielke (1978)	horizontal: 36 x 46 at 8km resolution vertical: levels defined at 10, 100, 500, 1000, 1500, 2000 m and so on.	20 hours
Rao & Agee 1996	Moeng-Purdue LES model (Moeng, 1984, 1986, and 1988) with ice phase	Lin et al (1983) Rutledge & Hobbs (1983) Murakami (1990)	horizontal 40 x 40 at 125m resolution vertical: 40 layers with 50m resolution	6000 seconds
Ballentine et al 1998	PSU-NCAR MM5 (Grell et al., 1994)	Dudhia (1989) with simplified treatment of ice and snow	horizontal: nested domains with resolution of 135, 45, 15 and 5km respectively vertical: 23 layers	36 hours
Cooper et al 2000	University of Oklahoma-Advanced Regional Prediction System (APRS) (Xue et al., 1995a,b)	Lin et al. (1983) Tao & Simpson (1993)	horizontal: 61 x 61 at 500m resolution vertical: 10m spacing near surface 200m spacing near and above the top of PBL	6 hours
Tripoli 2005	UW-NMS Tripoli (1992)	Bulk microphysics with cloud water, pristine ice crystals, aggregated crystals, and rimed crystals	horizontal: 500 x 90 at 400m vertical: 100m spacing inside lowest 1.2km, stretched slowly 750m spacing by 5km AGL	6 hours
Shi & Tao 2009	WRF v2.2.1	Goddard GCE Microphysics (Tao *et al.* 2003; Lang *et al.* 2007)	horizontal: 457 x 457 at 1km vertical: 61 layers	84 hours

Table 1 A list of numerical studies with cloud-resolving microphysics on lake-effect snowstorms.

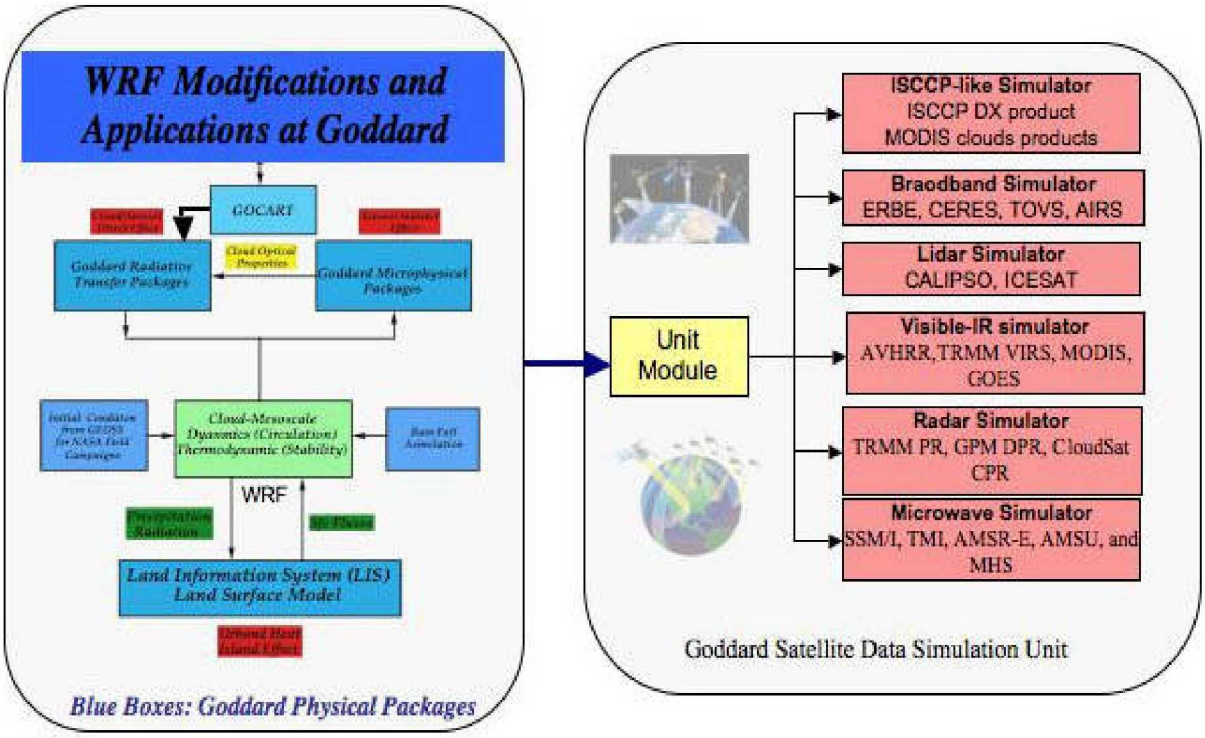

Fig. 1 (a) Physical packages added into WRF at Goddard. (b) Goddard Satellite Data Simulation Unit (SDSU).

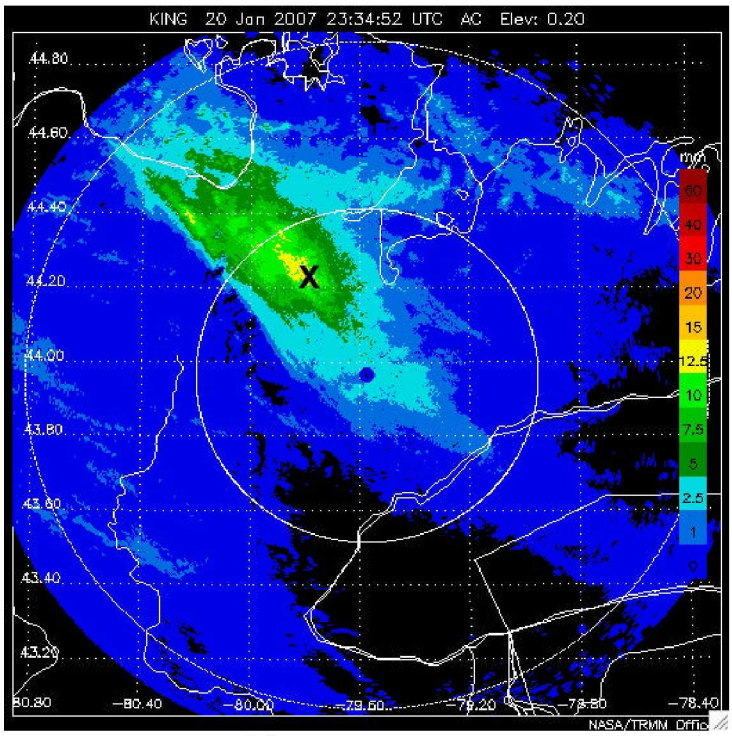

(a)

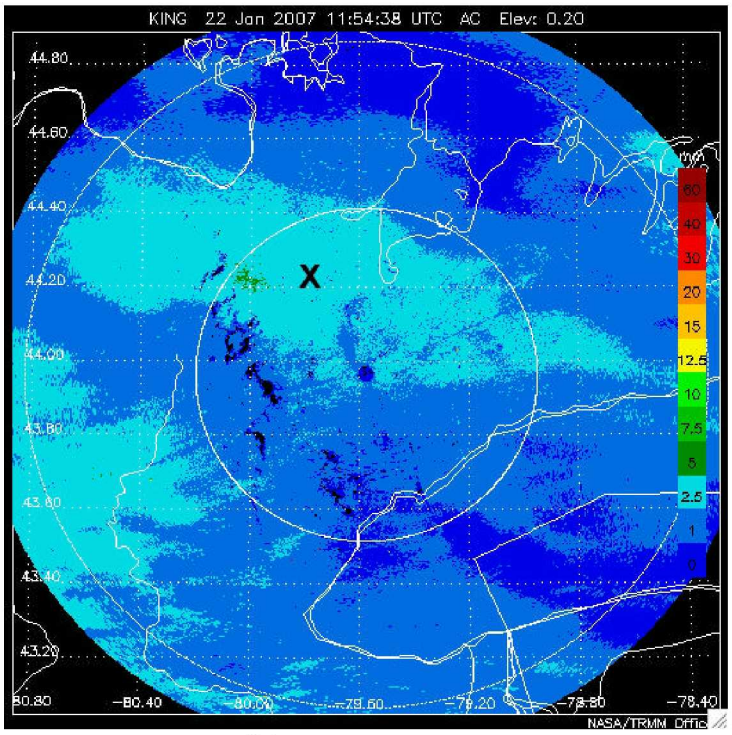

(b)

Fig. 2 24h-accumulated SR (liquid equivalent snow rate) for a) the lake event (00 UTC 20 to 00 UTC 21 January) and b) the synoptic event (12 UTC 21 to 12 UTC 22 January). "X" denotes the location of the CARE site.

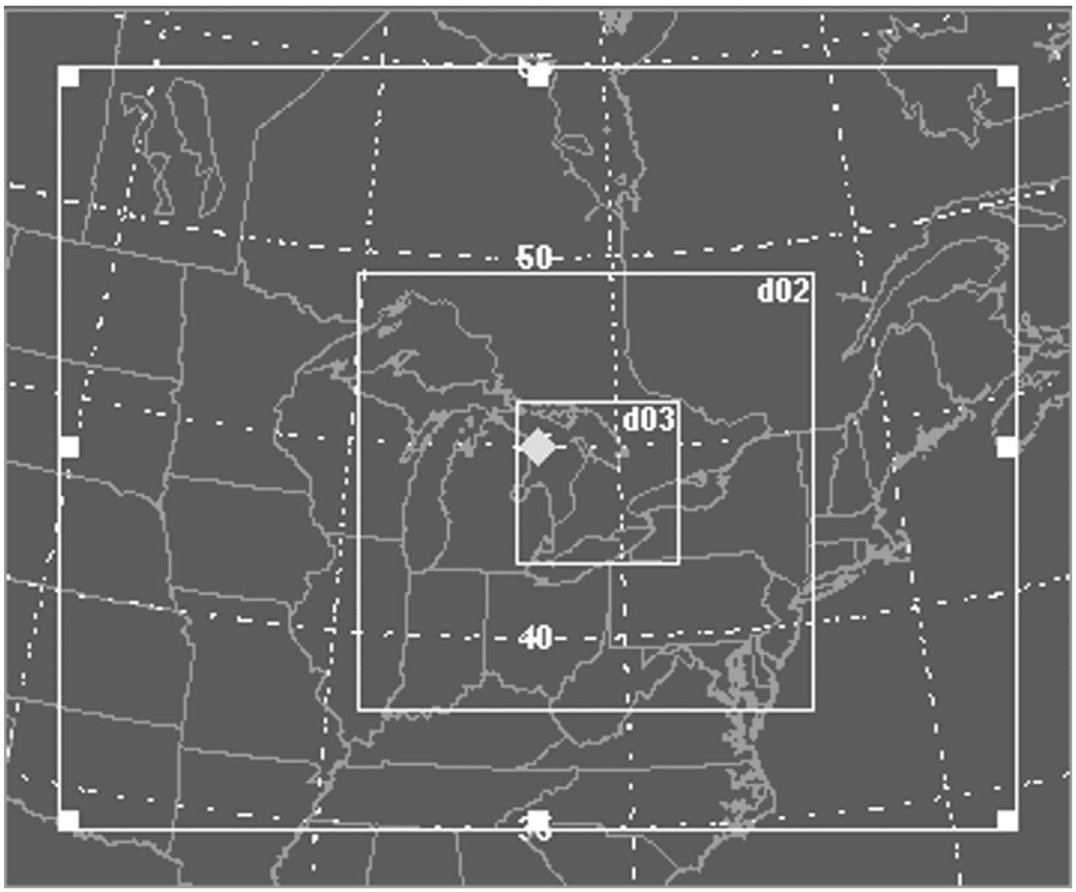

Fig. 3 Nesting configuration used for the C3VP simulations. Horizontal resolutions for domains 1, 2 and 3, are 9, 3 and 1 km, respectively.

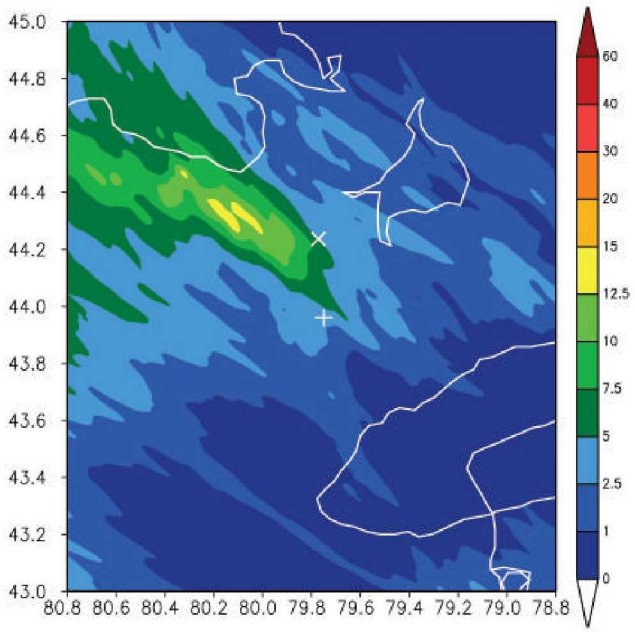

(a)

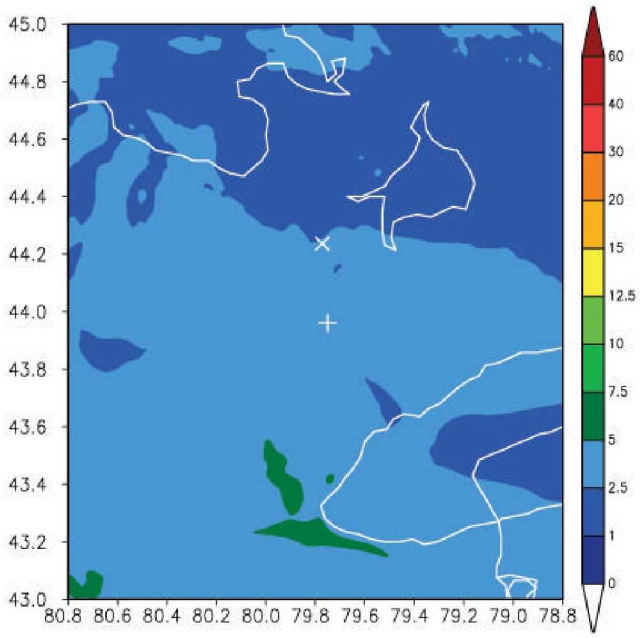

(b)

Fig. 4 24h-accumulated snowfall (mm, liquid water equivalent) for both events, (a) for the lake event (00 UTC 20 to 00 UTC 21 January), and (b) the synoptic event (12 UTC 21 to 12 UTC 22 January). "X" denotes the location of the CARE site and "+" denotes the location of King Radar.

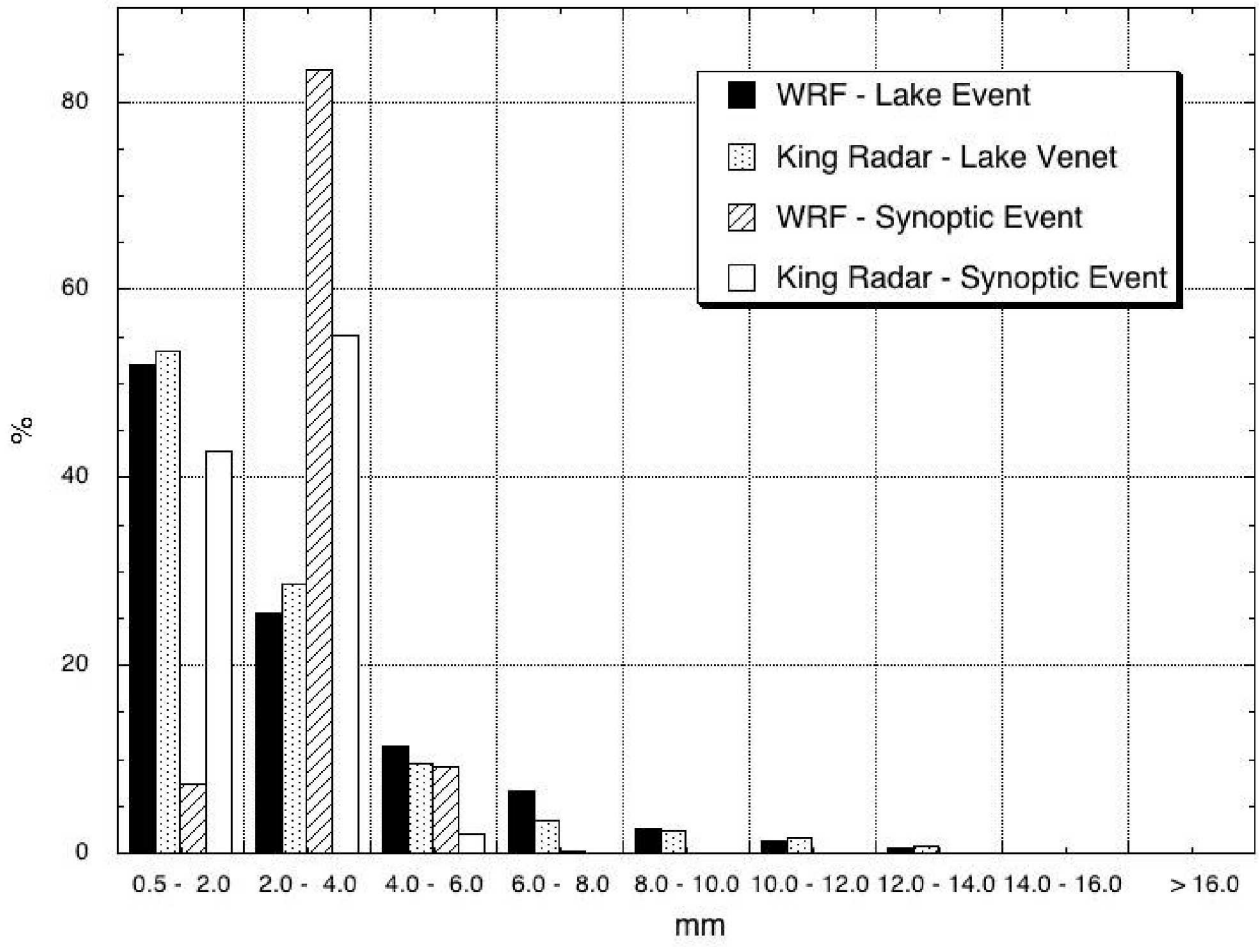

Fig. 5 PDF (probability distribution function) of 24h-accumulated snowfall (liquid equivalent). Results for the lake event were based on the data shown in Figs. 2a and 4a, while results for the synoptic event were based on the data shown in Figs. 2b and 4b.

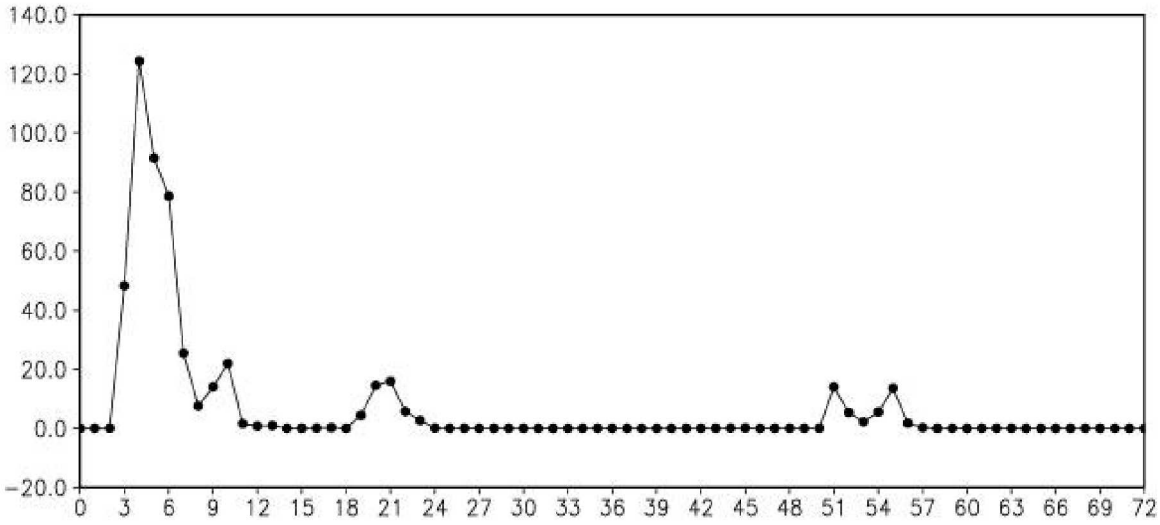

(a)

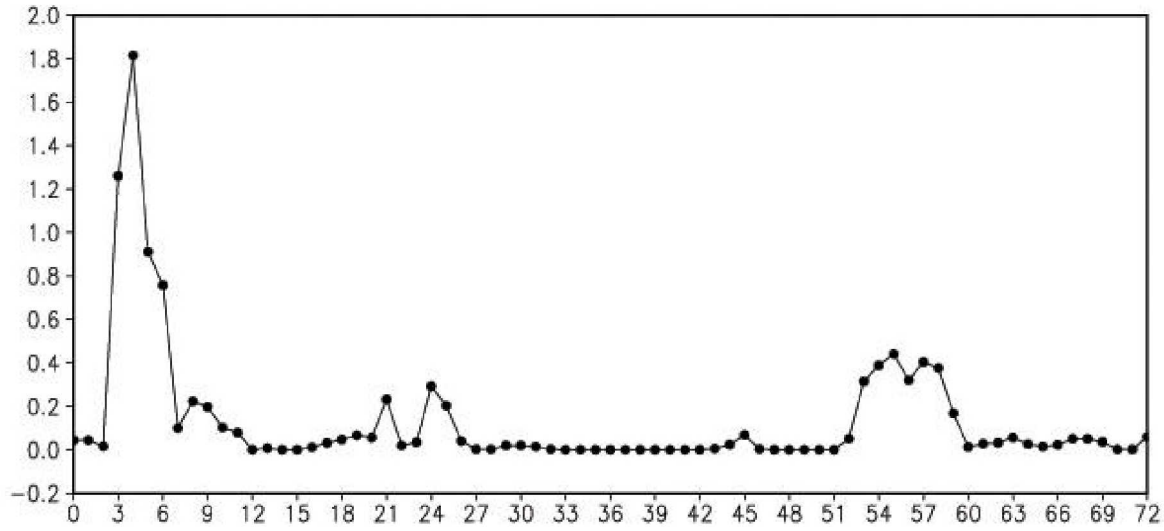

(b)

Fig. 6 (a) Snowfall rate (mm/hr, dry snow) collected from the Parsivel (Laser Optical) Disdrometer at the CARE site, (b) WRF simulated snowfall rate (mm/hour, liquid equivalent), between 00 UTC 1/20/2007 and 00 UTC 1/23/2007.

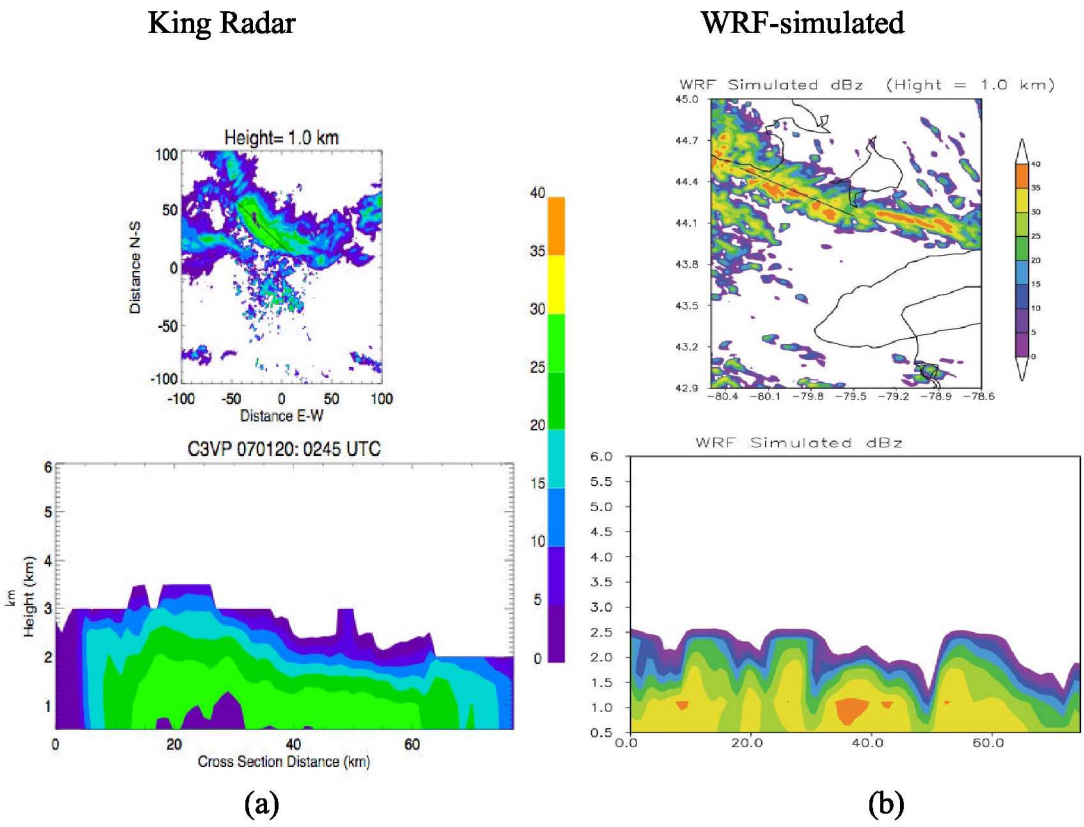

Fig. 7 Observations from King radar (a) are compared against the WRF simulated radar reflectivities (b) for the lake-effect event. The upper panels are the radar reflectivity at 1-km height centered at the King radar site (79.57W, 43.96N) and the slant lines show the location of the radar reflectivity cross-sections (lower panels).

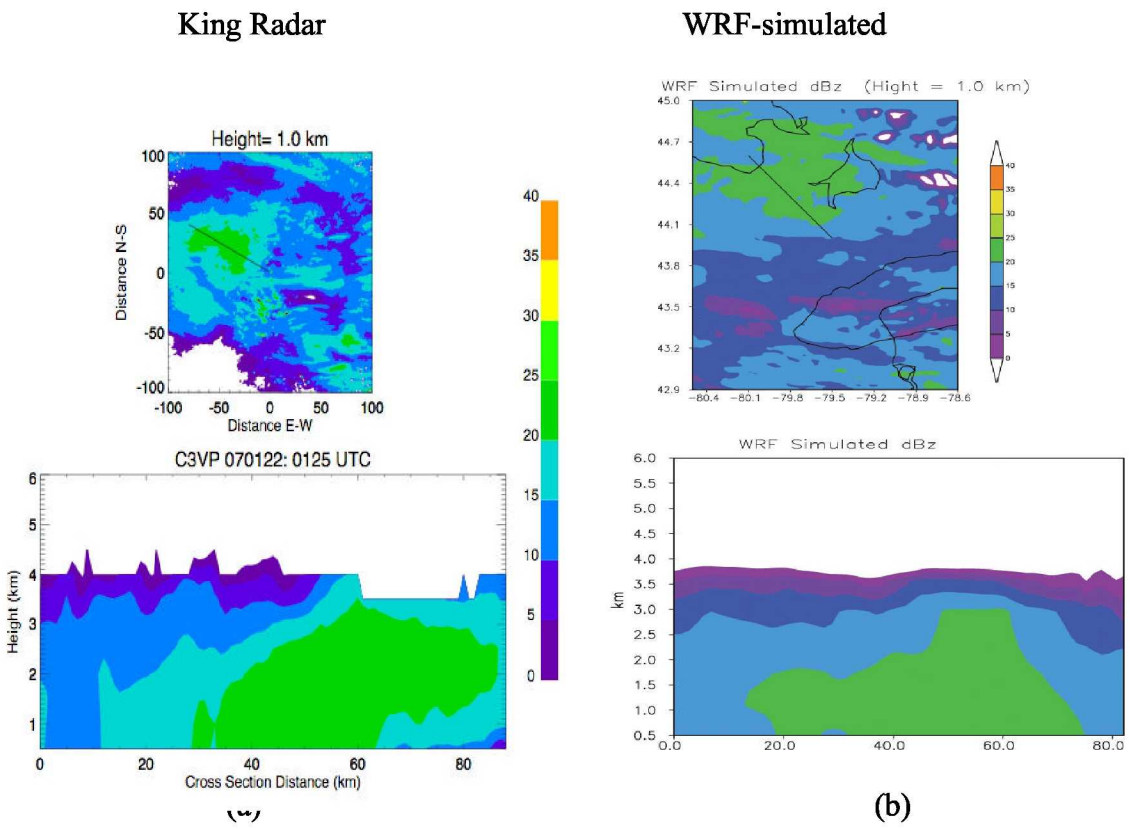

Fig. 8 Same as Fig. 7 except for the synoptic event.

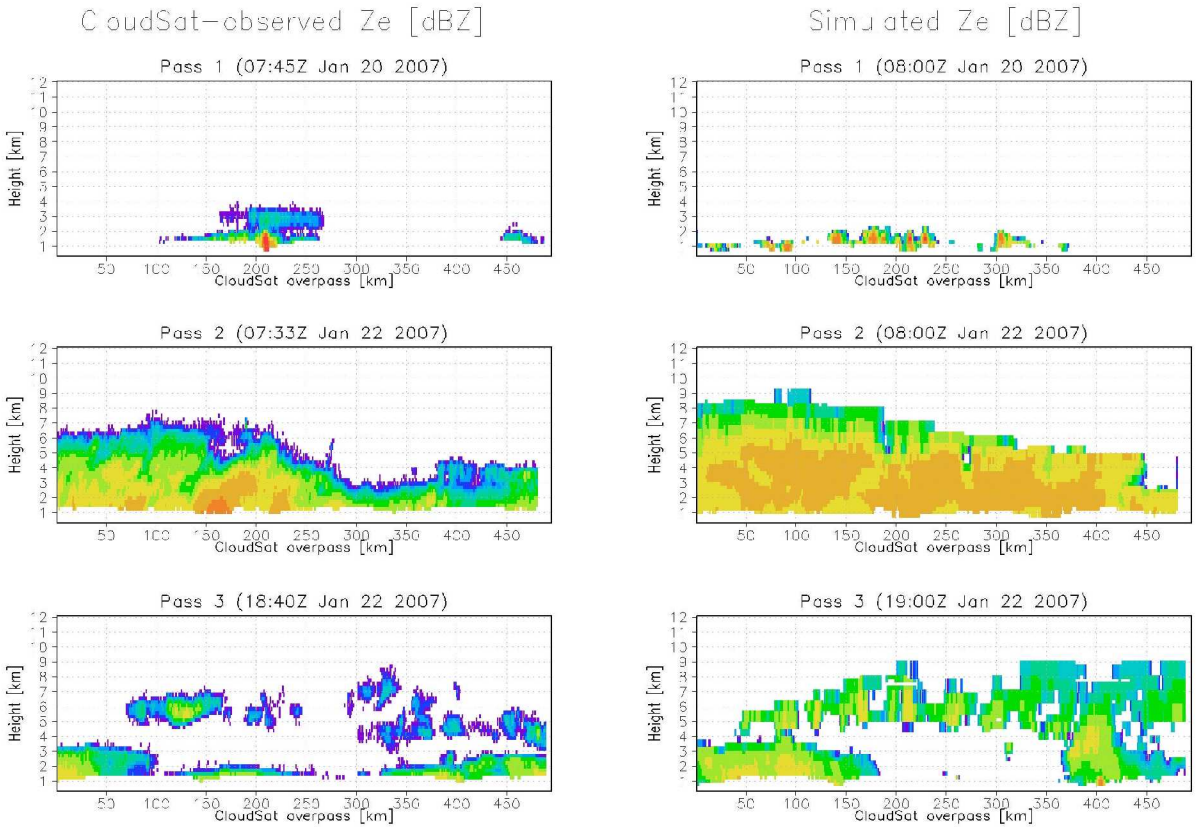

Fig. 9 Instantaneous cross-sections of CloudSAT-observed and WRF-SDSU-simulated Cloud Profiling Radar (CPR, 94 GHz) reflectivity. Left panels show the CloudSAT observations from three different passes and the right panels are the WRF-simulated.

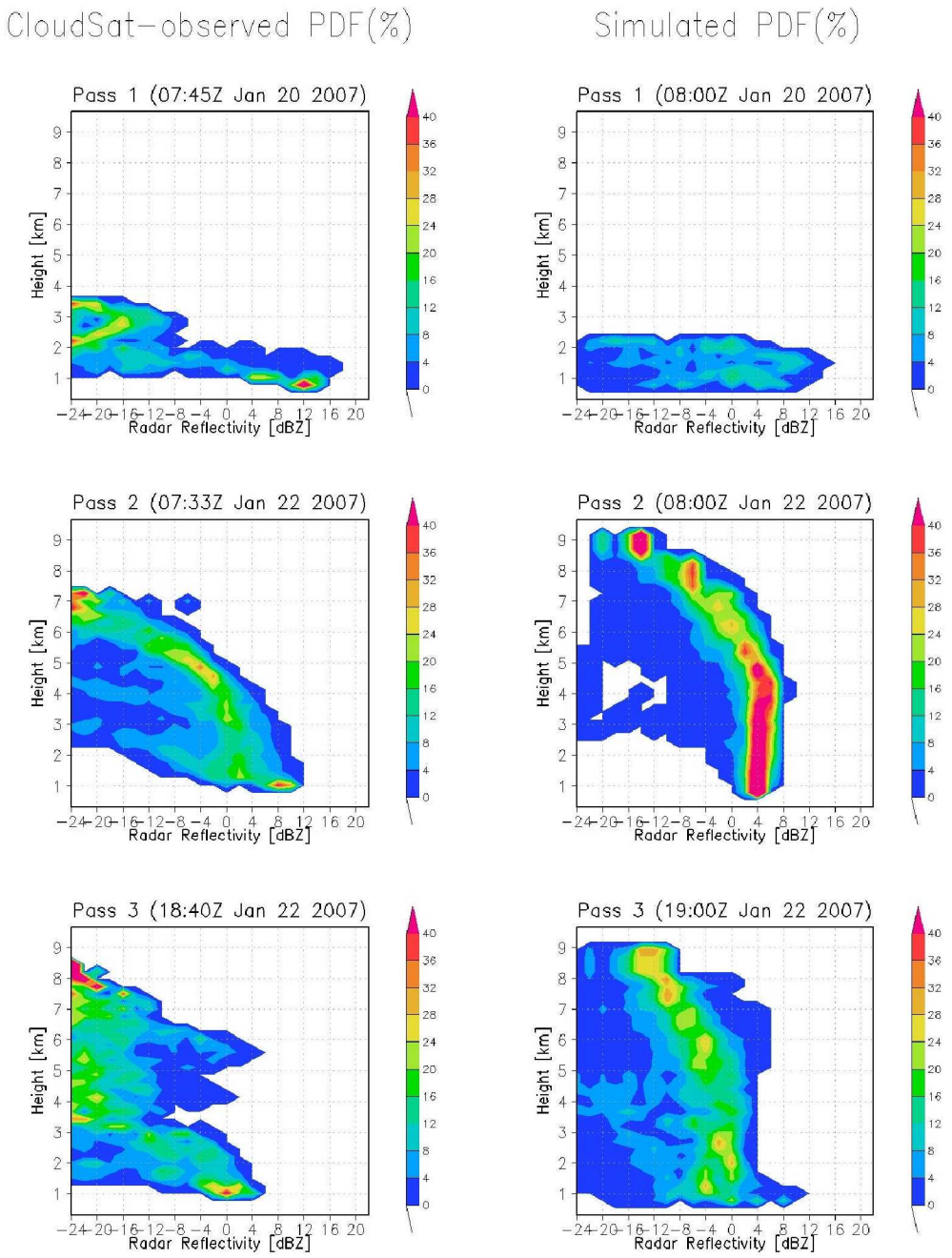

Fig. 10 Instantaneous contoured frequency with altitude diagrams (CFADs) of CloudSAT-observed and WRF-SDSU-simulated Cloud Profiling Radar (CPR, 94 GHz) reflectivity. Left panels show the CloudSAT observations from three different passes and the right panels are the WRF-simulated.

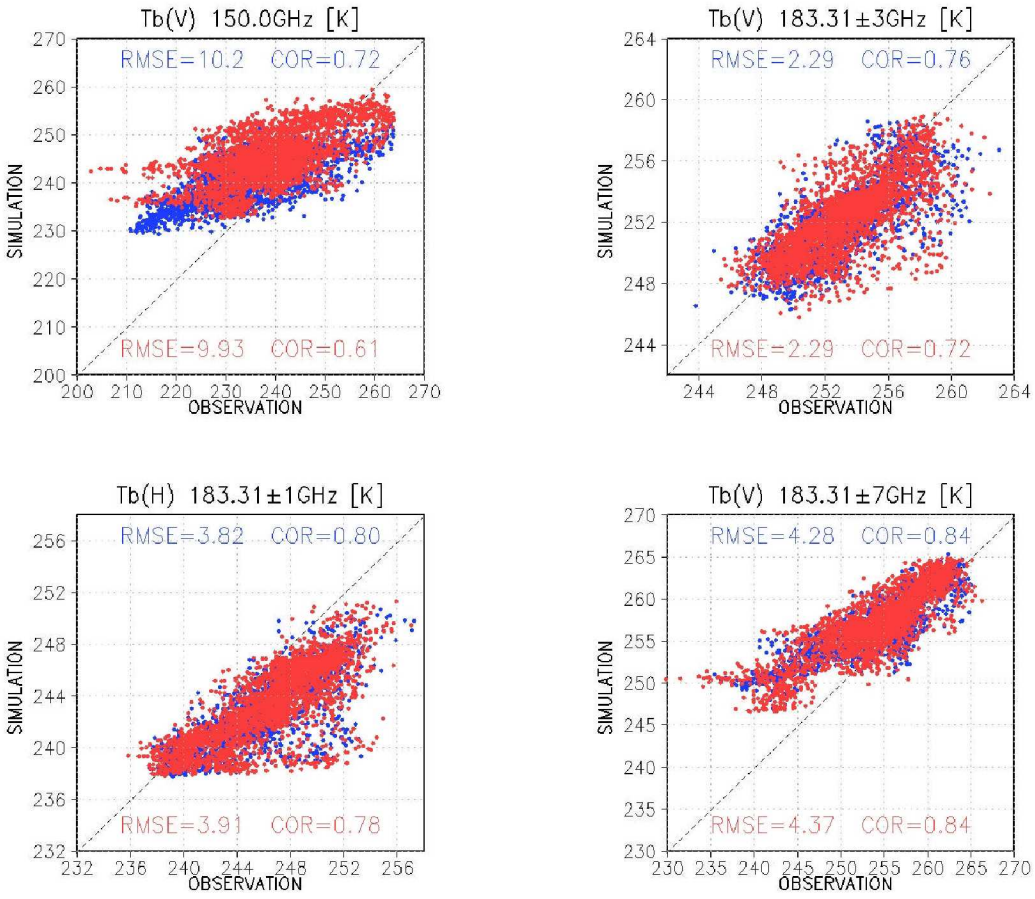

Fig. 11 Scatter plots between AMSU-B-observed and WRF-SDSU-simulated Tbs at different high-frequency channels. Red (blue) points represent over-land (water) points. Root Mean Square Error (RMSE) and correlation (COR) are also displayed.

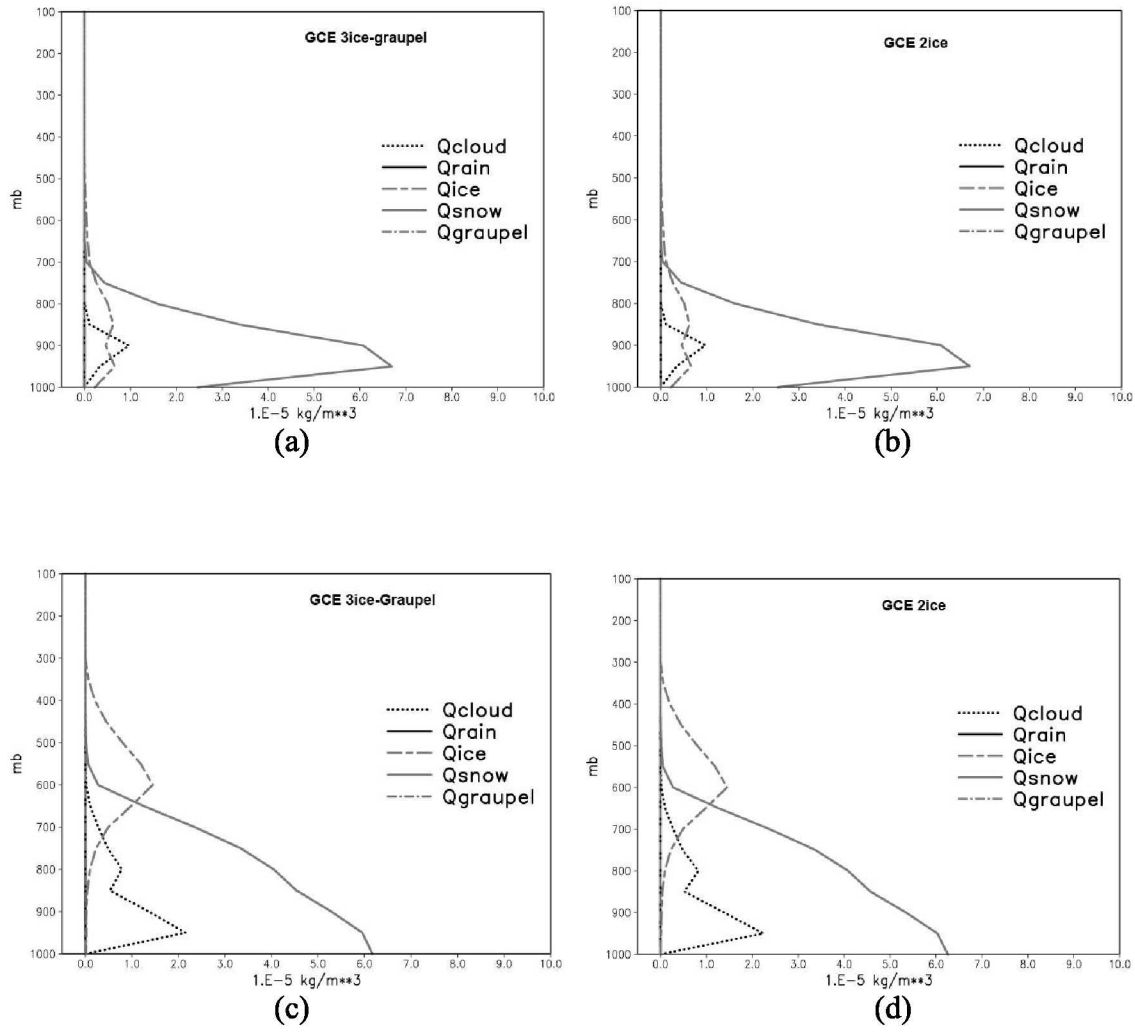

Fig. 12 WRF simulated vertical profiles of domain- and 24-hour time-average cloud species (i.e., cloud water, rain, cloud ice, and snow) for the lake event using (a) the GCE-3ice scheme, and (b) GCE-2ice scheme for the 24-hour period covering from 00UTC January 20 to 00UTC January 21, 2007, and for the synoptic event (c) the GCE-3ice scheme, and (d) GCE-2ice scheme for the 24-hour period covering from 00UTC January 21 to 00UTC January 22, 2007.

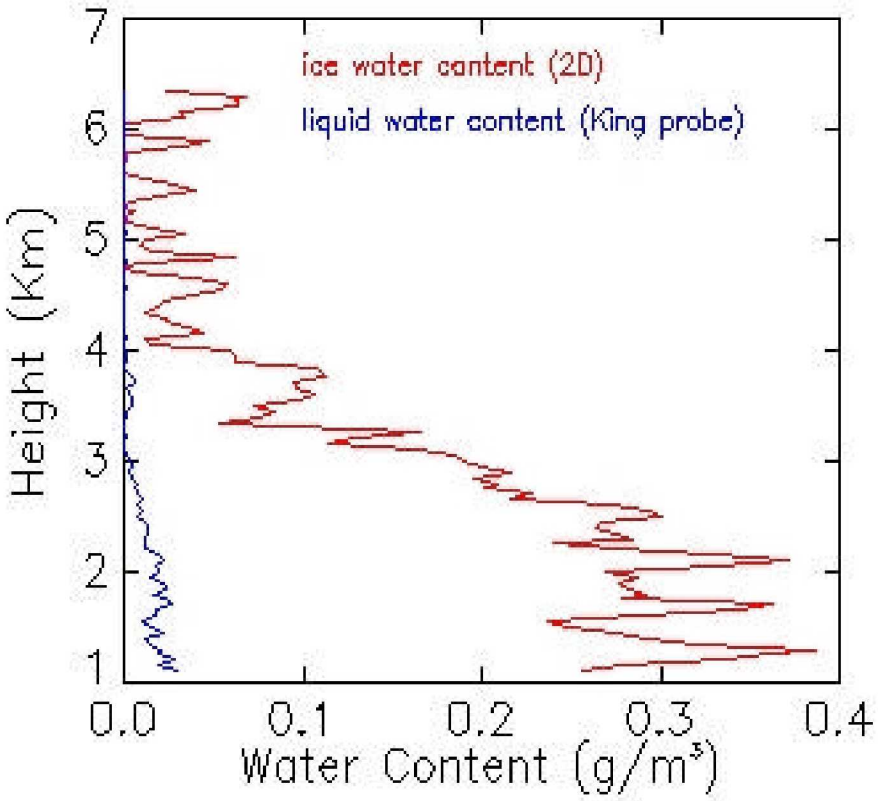

Fig. 13 Vertical profiles of C3VP aircraft measurement of ice and liquid water content between 0600UTC and 0624UTC January 22, 2007.

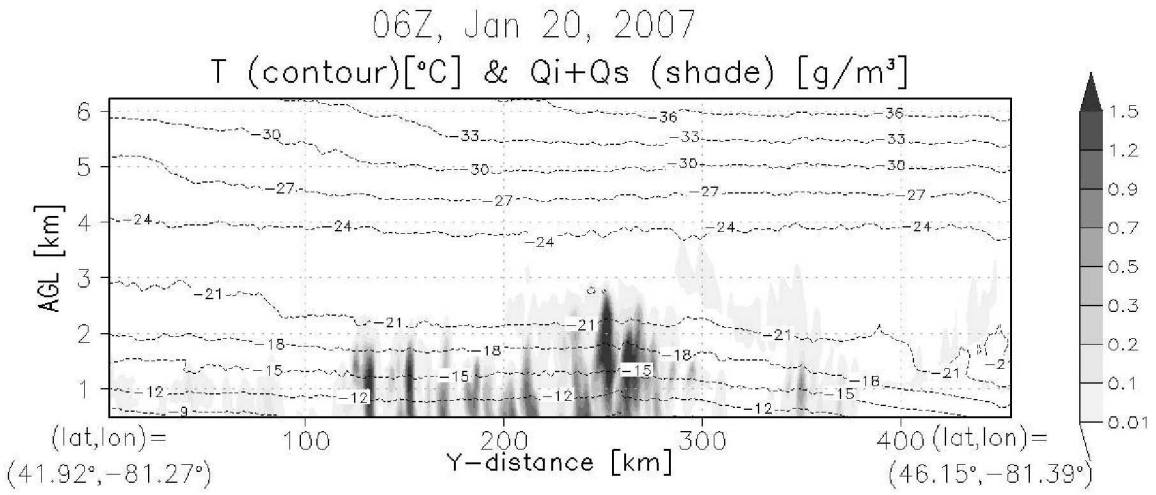

(a)

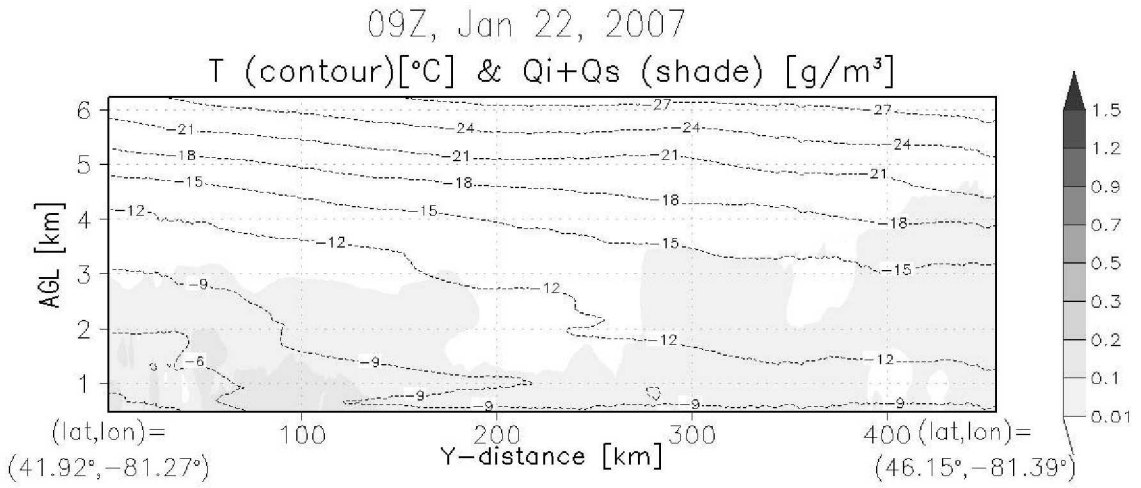

(b)

Fig. 14 WRF simulated temperature (^{0}C), cloud ice (g/m^3) and cloud snow (g/m^3) profiles for (a) the lake and (b) the synoptic events.

WRF Simulations of the January 20-22 2007 Snow Events over Eastern Canada: Comparison with in-situ and Satellite Observations

J. J. Shi, W.-K. Tao, T. Matsui, R. Cifelli, A. Hou, S. Lang, A. Tokay, C. Peters-Lidard, G. S. Jackson, S. Rutledge, and W. Petersen

J. Applied Meteor. Climatol.

Popular Summary

One of the grand challenges of the Global Precipitation Measurement (GPM) mission is to improve precipitation measurements in mid- and high-latitudes during cold seasons through the use of high-frequency passive microwave radiometry. For this, the Weather Research and Forecasting (WRF) model with the Goddard microphysics scheme is coupled with a Satellite Data Simulation Unit (WRF-SDSU) that has been developed to facilitate over-land snowfall retrieval algorithms by providing a virtual cloud library and microwave brightness temperature (Tb) measurements consistent with the GPM Microwave Imager (GMI). This study tested the Goddard cloud microphysics scheme in WRF for snowstorm events (January 20-22, 2007) that took place over the Canadian CloudSAT/CALIPSO Validation Project (C3VP) site up in Ontario, Canada.

In this paper, the performance of the Goddard cloud microphysics scheme both with 2ice (ice and snow) and 3ice (ice, snow and graupel) will be presented. The results are compared with King Radar data.

In addition, the WRF model output is used to drive the Goddard SDSU to calculate radiances and backscattering signals consistent with direct satellite observations for evaluating the model results. WRF simulations capture the basic cloud properties as seen by the ground-based radar and satellite (i.e., CloudSAT, AMSU-B) observations and also demonstrate the cloud streak feature in the lake event. This result also reveals that WRF was able to capture the cloud macro-structure reasonably well. The WRF-simulated cloud data set is available to the GPM science team through the Goddard Cloud library web site (http://portal.nccs.nasa.gov/cloudlibrary/).

Sensitivity tests utilizing both the 2ice (ice and snow) and 3ice (ice, snow and graupel) Goddard microphysical schemes were also conducted. The domain- and time-average cloud species profiles from WRF simulations with both microphysical schemes show identical results (due to weak vertical velocities and therefore the absence of large precipitating liquid or ice particles like graupel). However, both microphysics schemes produced an appreciable amount of liquid water while the C3VP aircraft measurements show there was much less liquid water than the model in both snow events. These results show that additional research is needed to improve the current cloud microphysics scheme for the extreme cold environment in high latitudes. Future aircraft observations are also needed to verify the non-existence of graupel in high-latitude in-land snow events.